

Optimal Bioreactor Operational Policies for the Enzymatic Hydrolysis of Sugarcane Bagasse

Inti Doraci Cavalcanti-Montañó · Carlos Alberto Galeano Suarez ·
Ursula Fabiola Rodríguez-Zúñiga · Raquel de Lima Camargo Giordano ·
Roberto de Campos Giordano · Ruy de Sousa Júnior

Published online: 22 January 2013
© Springer Science+Business Media New York 2013

Abstract The consolidation of the industrial production of second-generation (2G) bioethanol relies on the improvement of the economics of the process. Within this general scope, this paper addresses one aspect that impacts the costs of the biochemical route for producing 2G bioethanol: defining optimal operational policies for the reactor running the enzymatic hydrolysis of the C6 biomass fraction. The use of fed-batch reactors is one common choice for this process, aiming at maximum yields and productivities. The optimization problem for fed-batch reactors usually consists in determining substrate feeding profiles, in order to maximize some performance index. In the present control problem, the performance index and the system dynamics are both linear with respect to the control variable (the trajectory of substrate feed flow). Simple Michaelis–Menten pseudo-homogeneous kinetic models with product inhibition were used in the dynamic modeling of a fed-batch reactor, and two feeding policies were implemented and validated in bench-scale reactors processing pre-treated sugarcane bagasse. The first approach applied classical optimal control theory. The second policy was defined with the purpose of sustaining high rates of glucose production, adding enzyme (Accellerase® 1500) and substrate simultaneously during the reaction course. A methodology is described, which used economical criteria for comparing the performance of the reactor operating in successive batches and in fed-batch modes. Fed-batch mode was less sensitive to enzyme prices than successive batches. Process intensification

in the fed-batch reactor led to glucose final concentrations around 200 g/L.

Keywords Enzymatic hydrolysis · Cellulose · Bagasse · Sugarcane · Bioreactor · Fed batch

Nomenclature

| | |
|--------------------------|---|
| D | Dilution F_{feed}/V (per minute) |
| e | Enzyme concentration (in grams per liter) |
| $e_{\text{accumulated}}$ | Enzyme accumulated in the reactor (in filter paper unit) |
| e_{feed} | Enzyme to be added into the reactor (in filter paper unit) |
| F_{feed} | Substrate feeding flow rate (in liters per minute) |
| f_i | Process cash flow (in US dollars) |
| f_{i2} | Process cash flow per kilogram of treated bagasse (in US dollars per kilogram of bagasse treated) |
| H | Hamiltonian |
| J | Performance index |
| k | Rate constant of cellulose hydrolysis (per minute) |
| k_i | (Competitive) glucose inhibition constant (in grams per liter) |
| k_m | Michaelis–Menten constant (in grams per liter) |
| $M_{\text{accumulated}}$ | Accumulated mass of bagasse consumed (in grams) |
| P | Product concentration (in grams per liter) |
| P_0 | Initial product concentration (in grams per liter) |
| r | Reaction rate (in grams per liter per minute) |

I. D. Cavalcanti-Montañó · C. A. G. Suarez ·
U. F. Rodríguez-Zúñiga · R. de Lima Camargo Giordano ·
R. de Campos Giordano · R. de Sousa Júnior (✉)
Department of Chemical Engineering, Federal University of São
Carlos, Rod. Washington Luís, Km 235,
13565-905, São Carlos, SP, Brazil
e-mail: ruy@ufscar.br

| | |
|----------------------|--|
| r_{initial} | Initial reaction rate (in grams per liter per minute) |
| S | Cellulose (transformed in potential product concentration; in grams per liter) |
| S_{feed} | Substrate concentration in the feed (in grams per liter) |
| S_0 | Initial potential product concentration (in grams per liter) |
| t | Time (in seconds, minutes, or hours) |
| t_0 | Initial time (in seconds, minutes, or hours) |
| t_f | Final time (in seconds, minutes, or hours) |
| u | Control variable |
| V | Reaction volume (in liters) |
| V_0 | Initial reaction volume (in liters) |
| x | State variable |
| X | Substrate conversion |
| λ | Lagrange multiplier |

Introduction

Cellulosic residues (among them sugarcane bagasse) have an important positive feature as raw materials for liquid biofuels: they do not impact significantly the “food-versus-fuels” competition. An example is the production of second-generation (2G) bioethanol from sugarcane bagasse by the biochemical route, via the enzymatic hydrolysis of the biomass.

Sugarcane bagasse is a byproduct from the sugar and alcohol industry in Brazil. It consists of particles having a mean size of 20 mm, containing approximately 30 % of the cane mass and humidity around 50 % [1]. The bagasse composition depends on weather conditions and on the type of microorganisms to which the cane was exposed in the field. Banerjee and Pandey [2] report that sugarcane bagasse contains 32–48 % of cellulose, 19–24 % of hemicellulose, 23–32 % of lignin, and 3.2 to 5.5 % of ash.

The enzymatic hydrolysis of the cellulose present in the bagasse stems (the biomass C6 fraction) is due to the synergistic action of three groups of enzymes [3, 4]. Endoglucanases (or endocellulases) randomly attack amorphous regions within the polymeric chain, releasing reducing and nonreducing ends. These are then attacked by exocellulases or cellobiohydrolases (which are classified as of type I or II, as they attack reducing or nonreducing ends), releasing cellobiose. This, ultimately, has its β -1 \rightarrow 4 bonds hydrolyzed by β -glucosidase. This process is extremely complex and is affected by several factors: inhibitory effects by the products, nonproductive adsorption of the enzyme, mainly on the lignin still present after the pretreatment, resistance to mass transport, steric, and “jamming” effects [5, 6], among others. Thus, the kinetic modeling of the process is far from trivial, as described in Sousa Jr. et al. [7]. Many kinetic models have been developed for the enzymatic

hydrolysis of cellulose, but few are currently used in optimization or process control. Engineering practice for design and optimization has been based mainly on different empirical and semi-empirical approaches (nonmechanistic and semi-mechanistic models), including simple kinetic equations. Pseudo-homogeneous models, with two or three parameters, are frequently applied. They describe in very a simplified way the phenomena occurring in this complex system, but may show a good adherence to experimental data [7].

Cellulose hydrolysis using high loads of solids is an attractive alternative, reducing operation costs and water demands, and increasing the concentration of product [8]. Besides, the reduction of the impact of enzyme costs is still an important issue for the feasibility of the 2G-biochemical route, despite the recent progress towards cheaper enzyme cocktails.

Fed-batch reactors may minimize process costs. Yields and productivities may be increased using rational feed policies of substrates and catalysts to the reactor. Hodge et al. [9] developed an optimization strategy for cellulose hydrolysis for solid percentages higher than 15 %, when inefficient stirring and mixing in tank reactors may become a problem. Starting from a previously developed model for batch operation [10], and considering modifications to account for effects of feeding in fed-batch operation, a feeding policy (profile) was developed (based on optimal control theory) to maintain the insoluble solids concentration at a manageable level. Therefore, sugar concentration within the tank reactor may be increased without using a high initial load of insoluble solids.

In the work by Morales-Rodríguez et al. [11], three different feedback (PI) control strategies were developed and evaluated using a first-principles model of the hydrolysis process. A (re-calibrated) model of Kadam et al. [10] was used to test the performance of three control strategies.

In Chandra et al. [12], fed-batch hydrolysis experiments were conducted under the same conditions as batch hydrolysis with the exception that four loads of pre-treated substrates were added to the hydrolysis reaction at various specified times as opposed to adding all the substrate at the beginning of the reaction. All enzyme was added at the beginning of the reaction. Accessibility is a key factor governing the ability of the cellulases to catalyze the hydrolysis, and addition of a xylanase resulted in significant improvements in both hydrolysis yields and measured accessibility. The authors conclude that addition of ancillary enzymes or use of pretreatments that create more accessible substrates are required for an efficient hydrolysis at low enzyme loadings and high loads of solids.

More recently, Gupta et al. [13] carried out enzymatic hydrolysis at elevated solid loads (up to 20 %, w/v). A fed-batch strategy was implemented to enhance the final sugar concentration to 127 g/L. Batch and fed-batch enzymatic

hydrolysates were fermented with *Saccharomyces cerevisiae* and ethanol production of 34.78 and 52.83 g/L, respectively, were achieved.

In this work, two different feeding policies were designed, based on simple kinetic equations, and validated using bench-scale reactors. The first one feeds only the substrate to the semi-continuous reactor, and was defined using classical, off-line optimal control theory (here called policy (P)#1). The second policy (P#2) made use of both substrate and enzyme feeding, for sustaining high rates of glucose production.

Cash flows for these two strategies were assessed and compared with a series of sequential batches (policy P#3), taking into account the costs of the feedstock, of the catalyst and the prices of ethanol (in 2012, in Brazil). The methodology allowed evaluation of the best operational mode of the reactor (batch versus fed batch) using this metrics, for different scenarios with respect to the price of the enzyme.

Materials and Methods

Enzyme and Substrate

The commercial complex of cellulases Accellerase® 1500, from *Trichoderma reesei*, donated by Genencor® (Palo Alto, CA), was used. According to the manufacturer, this complex contains multiple enzymatic activities, different exoglucanases and endoglucanases, beta-glucosidase, and hemicellulase, too. This complex has its best operational stability between 50 and 65 °C and pH 4.0–5.0. However, in long-term assays, 50 °C is a better choice to minimize temperature inactivation. To determine the complex overall activity, the method of total reducing sugars was applied, making use of 3,5-dinitrosalicylic acid and Whatman filter paper No. 1 [14–16]. Enzymatic activity of the commercial pool of cellulases is $108 \text{ FPU g}^{-1}_{\text{enzyme complex}}$.

Steam-exploded sugarcane bagasse was donated by the Center for Sugarcane Technology (CTC—Piracicaba/SP).

Pretreatment Procedures

Steam-exploded bagasse was washed using a ratio of 1:20 (dry bagasse/boiling H₂O). Next, delignification was sought using a ratio of 1:20 (dry bagasse/NaOH solution 4 %, w/w), in autoclave for 30 min, at 1 atm and 121 °C. A high recalcitrance to enzymatic hydrolysis is frequently observed, particularly for sugarcane bagasse, when the removal of lignin is not carried out. The recalcitrance is due to the nonproductive adsorption of the enzyme to lignin. This is the reason why the delignification of steam-exploded sugarcane bagasse was carried out. After the removal of lignin, the remaining solid was thoroughly washed with hot water, being the last wash

carried out with 50 mM citrate buffer, pH 4.8. Table 1 shows the characterization of samples of steam-exploded bagasse before and after the pretreatment with NaOH. The analytical methodology for sugarcane bagasse was developed by Rocha et al. [17] and validated by Gouveia et al. [18]. The objective of the study presented in Gouveia et al. [18] was to validate the methodology described in Rocha et al. [17], for the chemical characterization of sugarcane bagasse. In Gouveia et al. [18], the methodology was validated through the analysis of results for characterization of the same sample of bagasse obtained by two different laboratories (in the Department of Biotechnology at Engineering School of Lorena and in the Department of Antibiotics at Federal University of Pernambuco).

The error associated with the characterization of pretreated sugarcane bagasse is around 3 % (the sum of percentages of cellulose, hemicellulose, lignin and ashes, both for steam-exploded sugarcane bagasse and for steam-exploded sugarcane bagasse treated with 4 % NaOH, is around 97 %, instead of 100 %). This margin of error (~3 %) is greater than the difference in percentage of ash contents between the non-delignified and delignified materials. Thus, the (unexpected) decline in the ash content in the delignified substrate must be due to experimental error.

Enzymatic Hydrolysis of Sugarcane Bagasse

Hydrolysis experiments were carried out in 200 mL-bench-scale-jacketed reactors, with mechanical stirring (Rushton impeller). Experiments were carried out in batch and fed-batch modes (with feeding policies detailed in the subsection “reactor modeling and optimization”). Initially (at the start-up of each run), 0.39 g of the enzymatic extract Accellerase® 1500 was added to each batch assay and into the P#2 fed-batch process (both in 37.3 mL of sodium citrate buffer, 50 mM, at pH 4.8). For fed batch with optimal control theory (in this case, only substrate feeding), 3.67 g of the same enzyme complex was initially added into the reactor (also in sodium citrate buffer). Pre-treated wet bagasse (15.56 g, with 82 % of humidity, i.e., 12.7 g of liquid phase), containing 70 % of cellulose (see Table 1), corresponding to a potential

Table 1 Characterization of pretreated sugarcane bagasse

| Samples | Cellulose (%) | Hemicellulose (%) | Lignin (%) | Ashes (%) |
|---|---------------|-------------------|------------|-----------|
| Steam-exploded sugarcane bagasse | 52.24 | 4.23 | 34.36 | 5.88 |
| Steam-exploded sugarcane bagasse, treated with 4 % NaOH | 70.12 | 3.79 | 19.32 | 4.25 |

glucose concentration of $44 \text{ g}_{\text{potential_glucose}} \text{L}^{-1} \text{solution}$ (in the reactor), was initially supplemented to the systems. Samples were collected from the supernatant for glucose analysis. Figure 1 shows the experimental setup. Table 2 summarizes the added enzyme and substrate for the three cases (P#1, P#2, and P#3). As one can see, final volumes for P#1 and P#2 were higher than the total capacity of one single bench-scale reactor. At this point, it must be explained that before the maximum capacity of one single reactor was achieved, the reaction medium was homogeneously divided (to avoid reactor flooding) into more than one single reactor (operating under the same conditions, off course).

Sugar Quantification

Glucose and cellobiose were determined by high-performance liquid chromatography using a Shimadzu SCL-10A chromatograph with detection by refractive index Shimadzu RID-10A, column Aminex HPX-87H ($300 \times 7.8 \text{ mm}$, Bio-Rad) with $0.005 \text{ molL}^{-1} \text{H}_2\text{SO}_4$ as mobile phase, at a flow rate of 0.6 mLmin^{-1} and oven temperature of $45 \text{ }^\circ\text{C}$.

Bioreactor Modeling and Optimization

The optimization problem for fed-batch reactors usually consists in determining substrate feeding profiles, in order to maximize some performance index. In optimal control theory [19], when the performance index and the system dynamics are both linear with respect to the control variable, the problem either results in bang-bang control or in a singular arc (intermediate) control.

Here, a simple Michaelis–Menten (MM) kinetic model with product inhibition, from Carvalho et al. [20], was applied for the dynamic modeling of the fed-batch reactor (as shown in Eqs. 1a–1d).

$$\frac{dS}{dt} = \frac{F_{\text{feed}} \cdot S_{\text{Feed}}}{V} - r - \frac{F_{\text{feed}} \cdot S}{V} \tag{1a}$$

$$\frac{dP}{dt} = r - \frac{F_{\text{feed}} \cdot P}{V} \tag{1b}$$

$$\frac{dV}{dt} = F_{\text{feed}} \tag{1c}$$

with

$$r = \frac{k \cdot e \cdot S}{k_m \cdot \left(1 + \frac{P}{k_i}\right) + S} \tag{1d}$$

Two feeding policies were defined in this work, and validated using bench-scale reactors. The first policy, P#1, predicts feeding of substrate but not of enzyme, and was defined using classical optimal control theory. The application of optimal control theory to our case leads to the set of equations that follows:

$$\frac{dx}{dt} = \underline{f}(x(t), \underline{u}(t), t) = \dot{x} = \underline{f}'(x) + \underline{g}(x) \cdot u \tag{2a}$$

Where

$$f' = \begin{bmatrix} -r \\ r \\ 0 \end{bmatrix}$$

$$g = \begin{bmatrix} (S_{\text{feed}} - S) \\ -P \\ V \end{bmatrix}$$

$$x = \begin{bmatrix} S \\ P \\ V \end{bmatrix}$$

$$u = D = F_{\text{feed}}/V$$

The inequality constrains are

$$u_{\text{min}} \leq u \leq u_{\text{max}} \text{ (with } u_{\text{min}}=0 \text{ and } u_{\text{max}}=F_{\text{feed max}}/V\text{)}.$$

The initial conditions are

$$x(0) = \begin{bmatrix} S_0 \\ P_0 \\ V_0 \end{bmatrix}$$

Fig. 1 Experimental apparatus for enzymatic hydrolysis

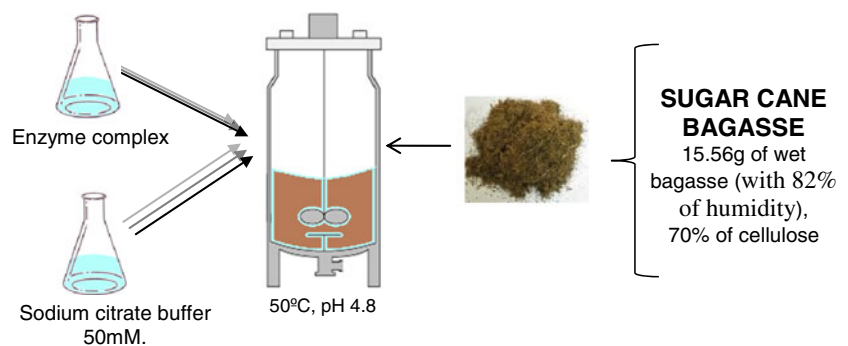


Table 2 Added enzyme and substrate for P#1, P#2, and P#3

| Feed policy | Initial enzyme added (g) | Total enzyme added (g) | Initial substrate added (cellulose transformed into potential glucose (g)) | Total substrate added (cellulose transformed into potential glucose (g)) | Initial volume (L) | Final volume (L) |
|------------------|--------------------------|------------------------|--|--|--------------------|------------------|
| P#1 ^a | 3.67 | 3.67 | 2.2 | 77.5 | 0.05 | 0.36 |
| P#2 ^a | 0.39 | 3.67 | 2.2 | 54.4 | 0.05 | 0.25 |
| P#3 ^b | 0.39 | 3×0.39 | 2.2 | 3×2.2 | 0.05 | 3×0.05 |

^aEight days of reactor operation^bThree batches of 2 days, two cleaning days

The performance index is minimized at a fixed final time:

$$J = -P(tf) - X(tf) \quad (2b)$$

where $X(tf)$ is the substrate conversion at the final time, see Appendix for the formulation of the problem.

In the present case, the singular arc does not exist, and then the only optimal control solution was a bang-bang strategy. Solving numerically the two-point boundary value problem encompassing the ordinary differential equations (in time) for the state (Eqs. 1a–1c) and co-state variables (Eq. 15), it is possible to determine the moment to switch the feed mass flow $u(t)$ between u_{\min} and u_{\max} .

The rationale behind the second feeding policy, P#2, was to pursue high rates of glucose production throughout the run, with the simultaneous addition of enzyme and substrate during the reaction course (Eqs. 3a–4). Extra enzyme must be loaded in order to compensate the inhibition of the old enzyme during the reaction course. At this point, it must be stressed that the reaction rate used to describe the kinetic behavior of the system (Eq. 1d) does not consider all the mechanisms that contribute for reducing the concentration of active enzymes in the system. In fact, the ineffective adsorption of enzyme on lignin, jamming effects (overcrowding of enzymes on the substrate matrix), inhibition by cellobiose, thermal inactivation of the enzymes, none of these phenomena are explicitly considered in the kinetic model. More than that, all enzymes of the pool are grouped in only one (pseudo)-catalyst. All these phenomena are nonetheless lumped in the constants of Eq. 1d, a pseudo-homogeneous model, and the significant point is that this simplified approach provided a good adherence to the experimental data. The model parameters were retuned using batch runs, and the acceptable accuracy of the model predictions for the fed-batch assays (see the “Results”) can be considered a positive validation test for this approach.

Policy P#2 is defined by the following equations:

$$e_{\text{feed}} = e \cdot V \cdot 108 - e_{\text{accumulated}} \quad (3a)$$

$$e = \frac{r_{\text{initial}} \cdot k_m \cdot \left(1 + \frac{P}{k_i}\right) + S_0}{k \cdot S_0} \quad (3b)$$

$$F_{\text{feed}} = \frac{r \cdot V}{S_{\text{feed}} - S_0} \quad (4)$$

Equations 3a–3b present the law to add additional quantities of enzyme, e_{feed} , to maintain a high reaction rate (close to r_{initial}) as the reaction proceeds, despite the formation of enzyme inhibitor (the product P). In Eqs. 3a–3b, the dimension of the enzyme concentration in the reactor (necessary to maintain r close to r_{initial}), e , is grams per liter; the dimension of enzyme to be added into the reactor, e_{feed} is filter paper unit. Therefore, “ e ” should be multiplied by the reactor volume (V) and by 108 (since 1 g of our enzyme complex is equivalent to 108 FPU). Besides, from the term “ $e \cdot V \cdot 108$ ” in Eq. 3a, it is necessary to subtract the enzyme already fed ($e_{\text{accumulated}}$) at the moment in consideration.

Equation 4, in turn, shows the substrate feeding flow rate, F_{feed} . It is calculated as a function of the rate of consumption of substrate, r (aiming that $dS/dt=0$, i.e., the substrate is replaced as it is consumed).

Results and Discussion

Initially, a validation of the MM model with product inhibition from Carvalho et al. [20] was done, using fresh experimental data obtained in batch mode. It is noteworthy

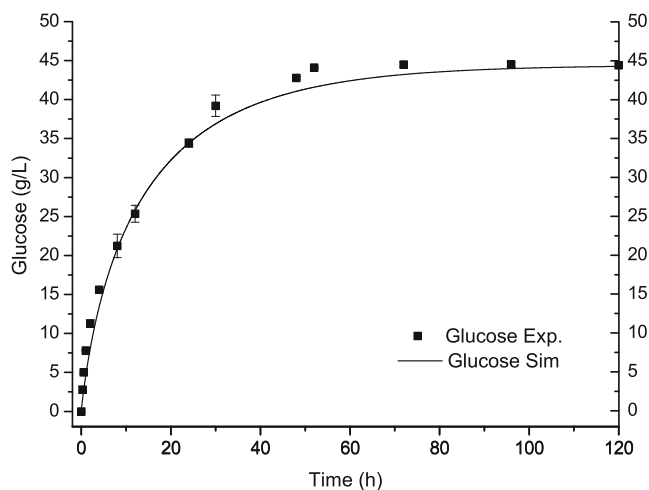


Fig. 2 Comparison of experimental and simulated data of batch operation. MM with inhibition parameters: $k_e=0.112 \text{ g L}^{-1} \text{ min}^{-1}$, $k_m=15 \text{ g L}^{-1}$, and $k_i=4.5 \text{ g L}^{-1}$. Error bars are standard errors of independent triplicate experiments. Operating conditions are 50 °C, pH 4.8, initial enzyme concentration $e(0)=7.8 \text{ g L}^{-1} \cong 842.4 \text{ FPUL}^{-1}_{\text{solution}}$ and initial potential glucose concentration of $44 \text{ g}_{\text{potential_glucose}} \text{ L}^{-1}_{\text{solution}}$

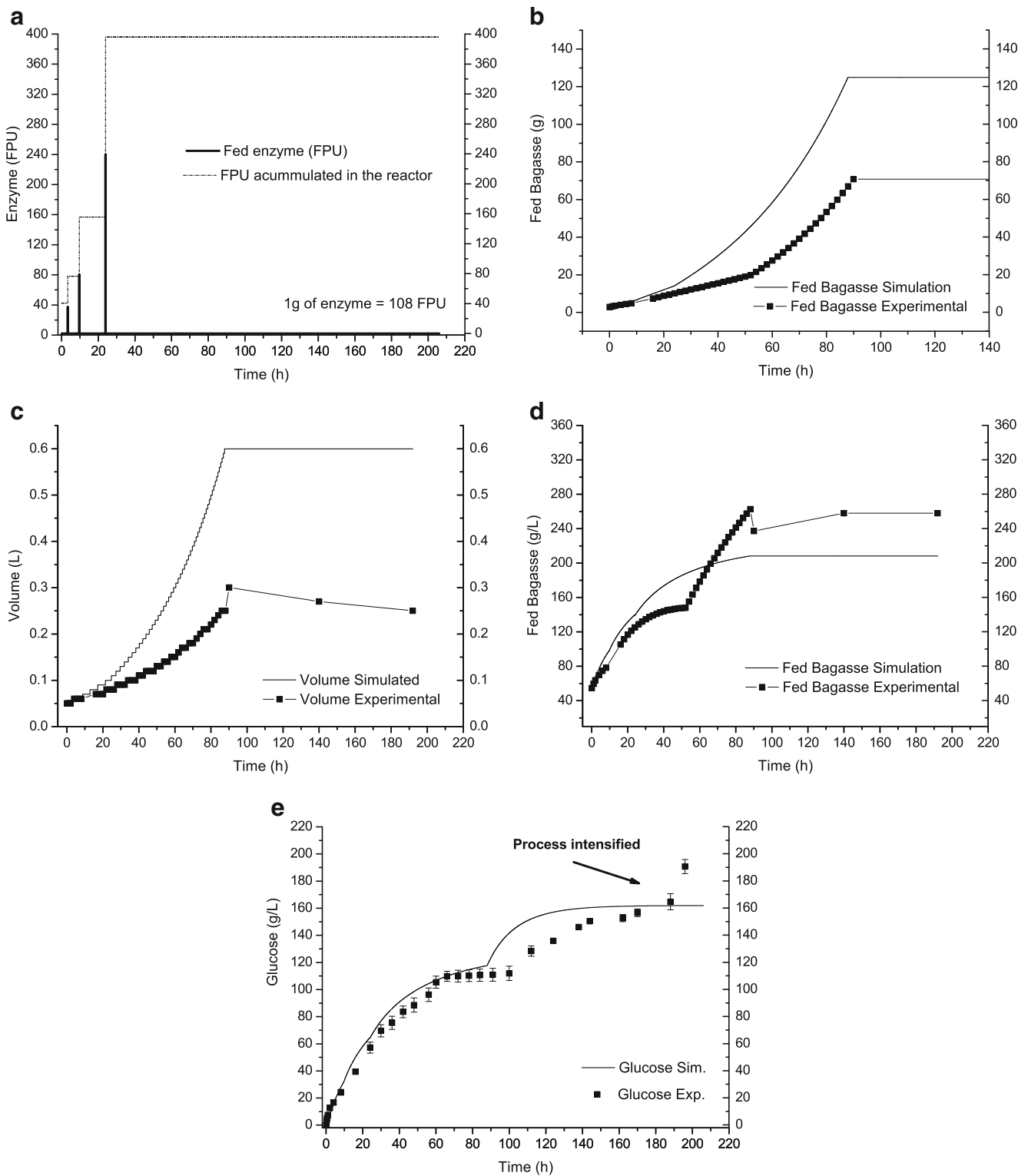


Fig. 3 **a** Fed enzyme (experimental equals simulated), operational policy P#2. **b** Experimental and simulated data for bagasse (operational policy P#2). **c** Experimental and simulated data for volume (operational policy P#2). **d** Experimental and simulated data for bagasse per volume (operational policy P#2). **e** Experimental and simulated data of glucose in fed-

batch operation (operational policy P#2). *Error bars* are standard errors of independent triplicate experiments. Operating conditions are 50 °C, pH 4.8, initial enzyme concentration $e(0)=7.8 \text{ g L}^{-1} \cong 842.4 \text{ FPUL}^{-1}$ solution and initial potential glucose concentration of $44 \text{ g}_{\text{potential_glucose}} \text{ L}^{-1}$ solution

that MM parameters ($k_e=0.105 \pm 0.015 \text{ g L}^{-1} \text{ min}^{-1}$, $k_m=8.78 \pm 4.89 \text{ g L}^{-1}$, and $k_i=3.34 \pm 1.30 \text{ g L}^{-1}$) from Carvalho

et al. [20] were obtained from assays in flasks under orbital shaking. In this work, the models are used for the

optimization of the operation of bench-scale reactors with impeller systems. Therefore, manual fine-tuning of some model parameters was tried. However, a good fit was obtained with parameters very similar to those from Carvalho et al. [20]. Figure 2 presents the results.

The dynamic model allowed evaluation of different operational modes of the reactor. Figures 3a–e show simulated and experimental results for the feeding policy P#2 (simultaneously adding enzyme and substrate during the reaction course).

The interruption of the substrate feeding occurred at around 87 h in the experimental assay, when a final batch process was carried out. This was the time in which the batch phase started in the simulations (see Fig. 3b). Due to the increase of the apparent medium viscosity, experimentally it was not possible to follow the simulated bagasse feeding profile, as seen in Fig. 3b. The reactor volume along time, is presented in Fig. 3c (experimental and simulated results). The main reason for the difference between experimental and simulated volumes was the lower addition of bagasse (and, consequently, of water from bagasse humidity) in the experimental assays. Besides, during the reaction course, evaporation of water from the system occurred. This is an intensification of the process since the concentration of glucose increased due to the hydrolysis reactions and to the evaporation of water. Evaporation contributed to experimental volume decrease (and, consequently, to the intensification of glucose concentration). This effect is more apparent from 90 h, when the feeding of substrate had stopped. The total decrease of volume during the final batch phase was of approximately 50 mL, due to evaporation. Figure 3d shows that when dividing the fed bagasse by the reactor volume, experimental and simulated situations become alike. The combined effects of evaporation and overestimation of the

theoretical reactor volume compensated the lower feeding of solid substrate, and high concentrations of glucose could be achieved (as shown in Fig. 3e).

The end of substrate feeding generated a discontinuity in the first derivative of glucose curves (Fig. 3e, mainly in the simulated results), which can be explained by the instantaneous reduction of the dilution effect caused by the feeding of new substrate.

It should be stressed that the long runs shown in these figures (almost 10 days) can certainly be reduced if greater enzyme loads were used. Of course, the final decision concerning the load of enzyme extract must be based on the economics of the process—operational costs of the reactor versus enzyme price. Nevertheless, the methodology herein is immediately applicable in any case. Having reliable models of the dynamics of the system, it is only a matter of simulating different start-up conditions in order to be able to discriminate which operational strategy should fit best in each case.

Figure 4a, b shows the comparison between experiments and simulated data for optimal control (P#1).

The experimental feeding of substrate for this policy could follow the calculated profile more closely, but the accumulation of solid residue in the reactor at the end of the feeding phase prevented the completion of the designed feed profile—the addition of bagasse had to be interrupted 3 h before expected. The addition of the enzyme cocktail followed the calculated profile. Despite the smaller amount of substrate added to the reactor, the concentration of glucose closely followed the simulated curve. Again, the intensification of the process due to evaporation of water (and the smaller addition of water, from the bagasse humidity) compensated the deprivation of substrate.

Figure 5 presents a comparison between our fed-batch feeding policies and successive batches, regarding the

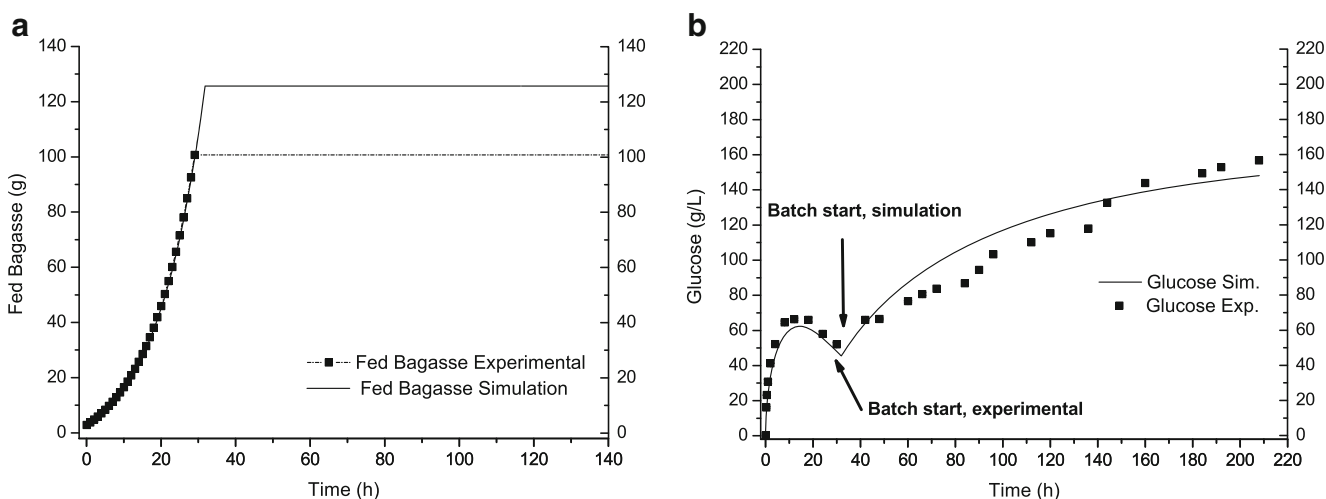


Fig. 4 **a** Experimental and simulated data for bagasse feeding for optimal control theory. **b** Experimental and simulated data for glucose during fed batch with optimal control. Operating conditions are 50 °C, pH 4.8,

initial enzyme concentration $e(0)=73.4 \text{ gL}^{-1} \equiv 7927.2 \text{ FPUL}^{-1}_{\text{solution}}$ and initial potential glucose concentration of $44 \text{ g}_{\text{potential_glucose}} \text{ L}^{-1}_{\text{solution}}$

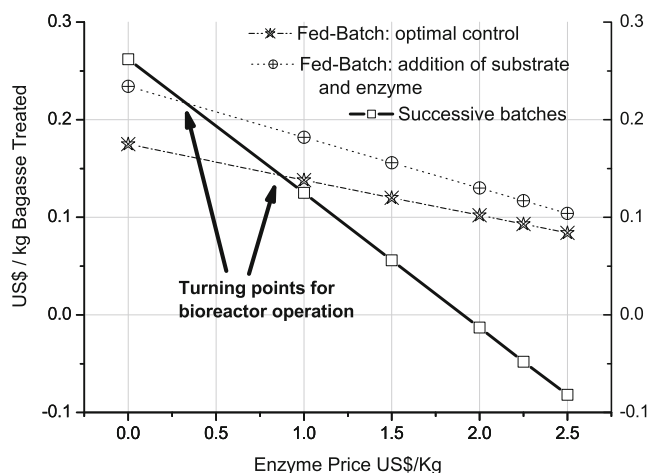


Fig. 5 Enzyme price sensitivity analysis

sensitivity with respect to the price of the enzyme. In Fig. 5, US dollar per kilogram of bagasse (treated), f_{i2} , was calculated according to Eqs. 5a–5b:

$$f_i = [\text{Ethanol price} \cdot (0.001) \cdot (0.46) \cdot P \cdot V] - [\text{Enzyme price} \cdot (0.001) \cdot \frac{M_{\text{accumulated}}}{108}] - [\text{Bagasse price} \cdot (0.001) \cdot M_{\text{accumulated}}] \tag{5a}$$

$$f_{i2} = \frac{f_i}{[(0.001) \cdot M_{\text{accumulated}}]} \tag{5b}$$

The term 0.46 in Eq. 5a transforms g of glucose into g of ethanol. The terms 0.001, in turn, are only to convert grams into kilogram. The term 108 is to convert FPU of enzyme into grams of enzyme. Both fed-batch policies, P#1 and P#2, are less sensitive to enzyme prices than the successive batches. For P#2, the enzyme price threshold was around US\$0.35/kg. This is valuable information for process operation. Except in a narrow portion of the enzyme price range, fed batch is better than batch.

Table 3 shows the comparison of simulated and experimental data for P#1, P#2, and P#3.

Policy P#2 (adding enzyme and substrate) led to higher glucose concentrations and cash flows. However, experimental

specific productivity for P#1 and P#2 was lower than those predicted by the simulations. This was due to the fact that less bagasse was fed during the experiments, for both situations, when compared with the simulations. Finally, it is important to say that overall mass balances for fed-batch (P#2) and batch (P#3) experiments in Table 3, taking into account the measurements of glucose and cellobiose, had errors of ~5 and ~0 %, respectively. For the feeding policy P#1, however, the quantification of glucose and cellobiose (per se) was not enough to close the overall mass balance since ~22 % of unconverted cellulose and oligosaccharides were still present at the end of the experiment (which is a further indicative that P#2 is the best feeding policy).

Conclusions

Three different strategies for the enzymatic hydrolysis of pre-treated sugarcane bagasse were compared: fed-batch operation adding only the substrate, according to the optimal control theory (P#1); fed-batch operation adding enzyme and substrate, with the goal of sustaining high reaction rates (P#2); and successive batches (P#3). The model-based strategies (P#1 and P#2) used simple pseudo-homogeneous kinetics to describe the rate of hydrolysis. All strategies were validated against experiments in bench-scale reactors. Sensitivity analyses were done using the price of the enzyme as parameter, with the purpose of evaluating the best operational mode for the reactor in different scenarios. The ad hoc fed-batch policy P#2 (adding enzyme and substrate), followed by the optimal control fed-batch P#1 provided better revenues than the series of batch runs for the present market values of enzyme, bagasse and ethanol in Brazil (in September 2012). However, there was a threshold where successive batches become advantageous, US\$0.35/kg_{enzyme}. Of course, these results are based only in a case study and have the sole purpose of demonstrating the utility of the tool.

Process intensification in a fed-batch reactor (adding enzyme and substrate simultaneously while the water naturally evaporates) led to glucose concentrations of approximately 200 gL⁻¹.

Table 3 Comparison of simulated and experimental data

| | P#1 ^a | | P#2 ^a | | P#3 ^b | |
|---|------------------|--------------|------------------|--------------|------------------|--------------|
| | Simulated | Experimental | Simulated | Experimental | Simulated | Experimental |
| Glucose concentration (gL ⁻¹) | 145.6 | 152.8 | 161.9 | 190.6 | 41.7 | 42.8 |
| Enz/glucose (g g ⁻¹) | 0.042 | 0.067 | 0.038 | 0.076 | 0.189 | 0.184 |
| Productivity (g _{glucose} L ⁻¹ h ⁻¹) | 0.758 | 0.794 | 0.843 | 0.992 | 0.217 | 0.223 |
| Specific productivity (g _{glucose} g _{enzyme} ⁻¹ h ⁻¹) | 0.124 | 0.078 | 0.138 | 0.068 | 0.028 | 0.028 |
| Cash flow (US\$/kg _{bagasse}) | 0.173 | 0.093 | 0.209 | 0.117 | -0.056 | -0.048 |

^aEight days of reactor operation

^bThree batches of 2 days, two cleaning days

Acknowledgments The authors would like to thank the support of Fundação de Amparo à Pesquisa do Estado de São Paulo (FAPESP-BIOEN), Conselho Nacional de Desenvolvimento Científico e Tecnológico (CNPq), Coordenação de Aperfeiçoamento de Pessoal de Nível Superior (CAPES) and CTC-Piracicaba for the steam-exploded bagasse.

Appendix

The first step in the development of the mathematical formulation of the optimal control algorithm is the dynamic description of the system to be controlled.

$$\frac{d\underline{x}}{dt} = \underline{f}(\underline{x}(t), \underline{u}(t), t) = \dot{\underline{x}} \quad (6)$$

Where $\underline{x}(t)$ is the vector of dimension n of state variables, at time t , $\underline{u}(t)$ is the control vector of dimension m , which specifies the input variables of the system model, \underline{f} is a vector of functions (the system model, in our case mass balances), and \underline{x} is the vector of state variables, calculated by the differential equations that constitute the model.

The purpose of the optimal control problem is to determine the control policy that will maximize or minimize a specific performance index, subject to restrictions imposed by the physical nature of the problem. The general performance index (functional) is:

$$J = h(\underline{x}(t_f), t_f) + \int_{t_0}^{t_f} F(\underline{x}, \underline{u}, t) dt \quad (7)$$

The necessary conditions for optimization in the presence of constraints are conveniently expressed in terms of the “Hamiltonian” (H); the performance index is maximized/minimized by maximizing/minimizing H :

$$\min_{\underline{u}(t), t_f} H = F(\underline{x}, \underline{u}, t) + \underline{\lambda}^T \underline{f}(\underline{x}, \underline{u}, t) \quad (8)$$

By applying the Maximum Principle of Pontryagin, a set of necessary conditions to maximize or minimize the functional are defined as:

$$\dot{\underline{\lambda}} = -\frac{\partial H}{\partial \underline{x}} \text{ Euler - Lagrange equation} \quad (9)$$

$$\dot{\underline{x}} = \underline{f} = \frac{\partial H}{\partial \underline{\lambda}} \text{ restrictions, the model} \quad (10)$$

$$\left[\frac{\partial h}{\partial \underline{x}}(t_f) - \underline{\lambda}(t_f) \right]^T \delta \underline{x}_f + (H(t_f) + \frac{\partial h}{\partial t}(t_f)) \delta t_f = 0 \text{ transversality} \quad (11)$$

$$\frac{\partial H}{\partial \underline{u}} = \underline{0} \text{ singular arc} \quad (12)$$

$$\dot{\underline{u}} = 0 \text{ bang-bang control} \quad (12')$$

In our case study, the performance index is minimized at a fixed final time:

$$J = -P(tf) - X(tf) = -P(tf) - \{[(S_0 \cdot V_0) + (S_{\text{feed}} \cdot (V(tf) - V_0)) - (S(tf) \cdot V(tf))]/[(S_0 \cdot V_0) + (S_{\text{feed}} \cdot (V(tf) - V_0))]\} \quad (13)$$

Through the Hamiltonian (H), the performance index could be maximized/minimized

$$H = \underline{\lambda}^T \cdot \left(\underline{f}(\underline{x}) + \underline{g}(\underline{x}) \cdot \underline{u} \right) = \lambda_1 \cdot [-r + (S_{\text{feed}} - S)D] + \lambda_2 \cdot (r - PD) + \lambda_3 \cdot (VD) \quad (14)$$

Applying the Euler–Lagrange equation:

$$\begin{aligned} \dot{\lambda}_1 &= \lambda_1 \cdot \left\{ D + (e \cdot k) / [S + k_m \cdot (P/k_i + 1)] - (S \cdot e \cdot k) / [S + k_m \cdot (P/k_i + 1)]^2 \right\} - \\ &\quad \lambda_2 \cdot \left\{ (e \cdot k) / [S + k_m \cdot (P/k_i + 1)] - (S \cdot e \cdot k) / [S + k_m \cdot (P/k_i + 1)]^2 \right\} \\ \dot{\lambda}_2 &= (-\lambda_1 \cdot S \cdot e \cdot k \cdot k_m) / \left\{ k_i \cdot [S + k_m \cdot (P/k_i + 1)]^2 \right\} + \\ &\quad \lambda_2 \cdot \left\{ u + (S \cdot e \cdot k \cdot k_m) / \left[k_i \cdot (S + k_m \cdot (P/k_i + 1))^2 \right] \right\} \\ \dot{\lambda}_3 &= -\lambda_3 \cdot u \end{aligned} \quad (15)$$

Finally, considering the transversality condition for fixed final time ($\delta t_f=0$) and free final conversion:

$$\begin{aligned}\lambda_1(t_f) &= V/[S_{\text{feed}} \cdot V + V_0 \cdot (S_0 - S_{\text{feed}})] \\ \lambda_2(t_f) &= -1 \\ \lambda_3(t_f) &= [S \cdot V_0 \cdot (S_0 - S_{\text{feed}})] / [S_0 \cdot V_0 + S_{\text{feed}} \cdot V - S_{\text{feed}} \cdot V_0]^2\end{aligned}\quad (16)$$

References

- Schilittler LAFS (2006) Engenharia de um bioprocesso para produção de etanol de bagaço de cana-de-açúcar. Dissertação (Mestrado em Ciências)—Escola de Química, Universidade Federal do Rio de Janeiro
- Banerjee R, Pandey A (2002) Bio-industrial applications of sugarcane bagasse: a technological perspective. *Int Sugar J* 104:64–67
- Walker LP, Wilson DB (1991) Enzymatic hydrolysis of cellulose: an overview. *Bioresour Technol* 36:3–14
- Woodward J (1991) Synergism in cellulase systems. *Bioresour Technol* 36:67–75
- Rothschild WG (1998) *Fractals in chemistry*. Wiley, New York
- Williams JC (2001) Macroscopic flow models. In: Gartner NH, Messer CJ, Rathi A (eds). Available from http://www.tft.pdx.edu/docs/revised_monograph_2001.pdf
- Sousa R Jr, Carvalho ML, Giordano RLC, Giordano RC (2011) Recent trends in the modeling of cellulose hydrolysis. *Braz J Chem Eng* 28:545–564
- Hodge DB, Karim MN, Schell DJ, Mcmillan JD (2008) Soluble and insoluble solids contributions to high-solids enzymatic hydrolysis of lignocellulose. *Bioresour Technol* 99:8940–8948
- Hodge DB, Karim MN, Schell DJ, McMillan JD (2009) Model-based fed-batch for high-solids enzymatic cellulose hydrolysis. *Appl Biochem Biotechnol* 152:88–107
- Kadam KL, Rydholm EC, McMillan JD (2004) Development and validation of a kinetic model for enzymatic saccharification of lignocellulosic biomass. *Biotechnol Prog* 20:698–705
- Morales-Rodríguez R, Capron M, Huusom JK, Sin G (2010) Controlled fed-batch operation for improving cellulose hydrolysis in 2G bioethanol production. In: 20th Eur Symp Comput Aided Process Eng—ESCAPE20
- Chandra RP, Au-Yeung K, Chanis C, Roos AA, Mabee W, Chung PA, Ghatora S, Saddler JN (2011) The influence of pretreatment and enzyme loading on the effectiveness of batch and fed-batch hydrolysis of corn stover. *Biotechnol Prog* 27:77–85
- Gupta R, Kumar S, Gomes J, Kuhad RC (2012) Kinetic study of batch and fed-batch enzymatic saccharification of pretreated substrate and subsequent fermentation to ethanol. *Biotechnol Biofuels* 5:16
- Miller GL (1959) Use of dinitrosalicylic acid reagent for determination of reducing sugar. *Anal Chem* 31:426–428
- Ghose TK (1987) Measurement of cellulase activity. *Pure Appl Chem* 59:257–268
- Adney B, Baker J (1996) Measurement of cellulase activities: chemical analysis and testing task. Laboratory analytical procedure. Available from <http://cobweb.ecn.purdue.edu/~lorre/16/research/LAP-006.pdf>
- Rocha GJM, Silva FT, Araújo GT, Curvelo AAS (1997) A fast and accurate method for determination of cellulose and polyoses by HPLC. In: Proceedings of the V Brazilian Symposium on the Chemistry of Lignin and Other Wood Components, vol. 5, pp. 113–115
- Gouveia ER, Nascimento RT, Souto-Maior AM, Rocha GJM (2009) Validação de metodologia para a caracterização química de bagaço de cana-de-açúcar. *Quím Nova* 32:1500–1503
- Ramirez WF (1994) *Process control and identification*. Academic, New York
- Carvalho ML, Sousa Jr R, Rodríguez-Zúñiga UF, Suarez CAG, Rodrigues DS, Giordano RC, Giordano RLC (2013) Kinetic study of the enzymatic hydrolysis of sugarcane bagasse. *Braz J Chem Eng* (in press)